Postprint of: Kulowski A., Analysis of a caustic formed by a spherical reflector: Impact of a caustic on architectural acoustics, Applied Acoustics, Vol. 165 (2020), 107333, DOI: 10.1016/j.apacoust.2020.107333

Analysis of a caustic formed by a spherical reflector:

Impact of a caustic on architectural acoustics

Andrzej KULOWSKI

Gdańsk University of Technology, Faculty of Architecture

ul. Gabriela Narutowicza 11/12, 80-233 Gdańsk, Poland; e-mail: kulowski@pg.edu.pl

Abstract

Focusing sound in rooms intended for listening to music or speech is an acoustic defect. Design recommendations provide remedial steps to effectively prevent this. However, there is a category of objects of high historical or architectural value in which the sound focus correction is limited or even abandoned. This also applies to indoor or outdoor concert shells, installations for teaching and acoustic presentations, etc. The main content of this article is deriving the equation of a caustic created by a concave hemispherical reflector with a source of rays situated at a given position. It is explained why under real conditions, both indoors and outdoors, no clear caustic resulting from the geometric approach is observed. Instead, its blurred form is perceived, usually limited to the caustic cusp taking the form of a point-like sound focus. This can be attributed to the effect of diffraction and interference, the impact of which on a caustic is analyzed in the paper.

Key words: spherical reflector; blurred focus; caustic; acoustic singularity; room acoustics; Rayleigh criterion

1. Introduction

Large curved surfaces in a form of arched vaults and concave walls are often found in historical buildings as well as in modern buildings. In most cases, their presence in historical buildings results from structural and cultural conditions, becoming an element of an architectural style. Large curved surfaces can also be found in contemporary facilities. They may cause the phenomenon of sound concentration, which is unfavorable to room acoustics. When it occurs in an existing rooms, especially those intended for listening to speech or music, the effect of sound concentration is effectively corrected. Also, when designing halls for this purpose, the measures are taken in advance to prevent sound concentration like avoiding large concave surfaces, using sound diffusing structures, etc. A separate problem is the unintended focusing effect, discovered accidentally at an unusual location of the sound source and the observer, which happens even in halls with a high reputation. These issues are recognized in detail in the literature and design recommendations and are not the subject of this article [1]. However, in objects with a high historical value, or when acoustic quality is not a basic element of its function, etc. the sound focusing effect is usually not corrected. This also applies to interiors where an accidentally discovered acoustic effect becomes a tourist attraction or when the effect of sound concentration is created intentionally, e.g. in concert shells in halls or facilities with this function in the open air. It also happens that the sound concentration effect is created deliberately for educational purposes, both in historical times and today [2].

In most cases, the literature on architectural acoustics tacitly acknowledges that the sound concentration caused by large curved elements of walls or ceilings has a compact, almost point-like form. It only applies to a few specific cases, among them a source in the center of a spherical reflector, a parabolic reflector with a source on a geometric axis, or an ellipsoidal reflector with a source in one of its focuses.

The phenomenon of the formation of a focus in a geometrically predictable shape called caustics has been known for several centuries. E.g., numerous drawings of caustics can be found in Leonardo da Vinci's sketches related to his research in the field of optics between 1510-1515 [3]. In modern times, the formation of a caustic is the subject of mathematical studies [4-6], and a caustic is pre-

sent in many fields of technology and science, mainly regarding light or sound propagation, e.g. hydroacoustics, aeroacoustics, ultrasound and laser technology, and even deep space cosmology [7-9].

Research on a caustic usually assumes that the source of rays is a point in infinity which means that the beam consists of parallel lines [2], [10], [11]. This article discusses the case where the source is at a specific distance from the reflector, whereby the rays form a divergent bundle. The derived formula applies to the source placed inside or outside the bowl of the reflector. As a limit case, a bundle of parallel rays corresponding to an infinitely distant source is also considered.

In addition to the mathematical analysis of the formation of caustics, the purpose of this article is to explain why in real conditions, both indoors and outdoors, instead of geometrically predicted forms of caustics their blurred form is observed. When the mirror is in the free field, this can be attributed to the interference of the incident wave with the wave that forms the caustics and the wave deflection at the mirror edges. These phenomena are analyzed in the article. In rooms, focusing effect is additionally masked by the wave reflections of the higher order, which are also subject to the aforementioned wave effects.

The article discusses the following issues: geometrical analysis of caustics (Section 2), assessment of energy distribution over a caustic (Section 3), the impact of wave effects on a caustic in the field of acoustics (Section 4) and examples of caustics in rooms and in open space (Section 5).

2. Caustics created by the concave spherical reflector

In this chapter a formula is derived which describes the axial section of the caustic with a source of rays located at a specified position on and outside the symmetry axis of the reflector and an infinitely distant source as the limit case.

Consider a bundle of rays emitted from point S located at a distance d from the concave spherical reflector (Fig. 1). The reflected ray ℓ_r is described by a straight line (1)

$$y=ax+b \tag{1}$$

where

$$a = \mathrm{tg}(\varphi-\theta) \tag{2}$$

is the slope of the line. Since the reflection point, M(Rcos(θ),-Rsin(θ)) belongs to the straight line ℓ_r , substitution of x and y by Rcos(θ) and -Rsin(θ), respectively, gives the factor b in Eq. (1)

$$b = y-ax = -R\sin(\theta) - tg(\varphi-\theta)\, R\cos(\theta) \tag{3}$$

After inserting a and b into Eq.(1), the line ℓ_r is in the form

$$y(x,\theta,\varphi) = tg(\varphi-\theta)(x-R\cos(\theta)) - R\sin(\theta) \tag{4}$$

The caustic is formed by the rays tangent to it, so the variation of the slope of the line ℓ_r due to infinitesimally small changes of the angle φ tends to zero. Hence, the derivative of the Eq. (4) over φ must equal 0:

$$dy/d\varphi=0. \tag{5}$$

Since y in Eq. (4) is a function of variables φ and θ, its derivative over φ may be written as:

$$\frac{dy}{d\varphi} = \frac{\delta y}{\delta \varphi} + \frac{\delta y}{\delta \theta} \times \frac{\delta \theta}{\delta \varphi} = 0 \tag{6}$$

The solution to equation (6) is y (φ), which is then transformed into the form y(x,θ). The functions x(θ) and y(x,θ) form a parametric description of a caustic. The steps for this procedure are shown in equations. (7) - (15c). Details of mathematical transformations are shown in Appendix 1

The sine and cosine rules (Eq.(7) and (9), respectively) applied to the SOM triangle in Fig. 1 are converted to Eq. (8) and (10):

$$\frac{R}{\sin(\Pi/2 - (\theta+\varphi))} = \frac{d}{\sin(\varphi)} = \frac{c}{\sin(\Pi/2+\theta)} \quad \rightarrow \quad \frac{\cos(\theta+\varphi)}{R} = \frac{\sin(\varphi)}{d} = \frac{\cos(\theta)}{c} \tag{7), (8}$$

$$c^2 = R^2 + d^2 - 2Rd\cos(\Pi/2+\theta) \qquad c = \sqrt{R^2 + d^2 + 2Rd\sin(\theta)} \tag{9), (10}$$

The combination of the above equations yields the functions $\theta(\varphi)$ and $\varphi(\theta)$ (see Eq. (11) - (13), respectively).

$$\theta(\varphi) = \arccos\left(\frac{R\sin(\varphi)}{d}\right) - \varphi \qquad \varphi(\theta) = \arccos\left(\frac{R\cos(\theta)}{\sqrt{R^2 + d^2 + 2Rd\sin(\theta)}}\right) - \theta \tag{11), (12}$$

$$\varphi(\theta) = \arcsin\left(\frac{d\cos(\theta)}{\sqrt{R^2 + d^2 + 2Rd\sin(\theta)}}\right) \tag{13}$$

After inserting Eq. (13) into Eq. (4) and calculating partial derivatives in Eq. (6), Eq. (5) takes the form (14) (see Appendix 1, Eq. (A1.4)).

$$\frac{dy}{d\varphi} = \frac{x - R\cos(\theta)}{\cos^2(\varphi-\theta)}\left(2 + \frac{R\cos(\varphi)}{\sqrt{d^2 - R^2\sin^2(\varphi)}}\right) - R\left(\mathrm{tg}(\varphi-\theta)\sin(\theta) - \cos(\theta)\right)\left(1 + \frac{R\cos(\varphi)}{\sqrt{d^2 - R^2\sin^2(\varphi)}}\right) = 0 \tag{14}$$

Extracting the variable x from Eq. (14) and presenting Eq.(4) in the form y(θ) with the use of Eq. (12) and (13) yields the system of equations (15a)-(15c) (see Appendix 1, lines (A1.18) and (A1.19)).

$$\begin{cases} x(\theta) = R\left(-\cos(\theta) + \sin(\theta)\times \mathrm{tg}\left(\Gamma(\theta)\right)\right)\times\cos^2\left(\Gamma(\theta)\right)\times\dfrac{R^2 + d^2 + 2Rd\sin(\theta)}{R^2 + 2d^2 + 3Rd\sin(\theta)} + R\cos(\theta) & \text{(15a)} \\ y(x,\theta) = \left(x(\theta) - R\cos(\theta)\right)\mathrm{tg}\left(\Gamma(\theta)\right) - R\sin(\theta) & \text{(15b)} \end{cases}$$

$$\text{where } \Gamma(\theta) = \arcsin\left(\frac{d\cos(\theta)}{\sqrt{R^2 + d^2 + 2Rd\sin(\theta)}}\right) - \theta, \qquad 0 \le \theta \le \Pi \tag{15c}$$

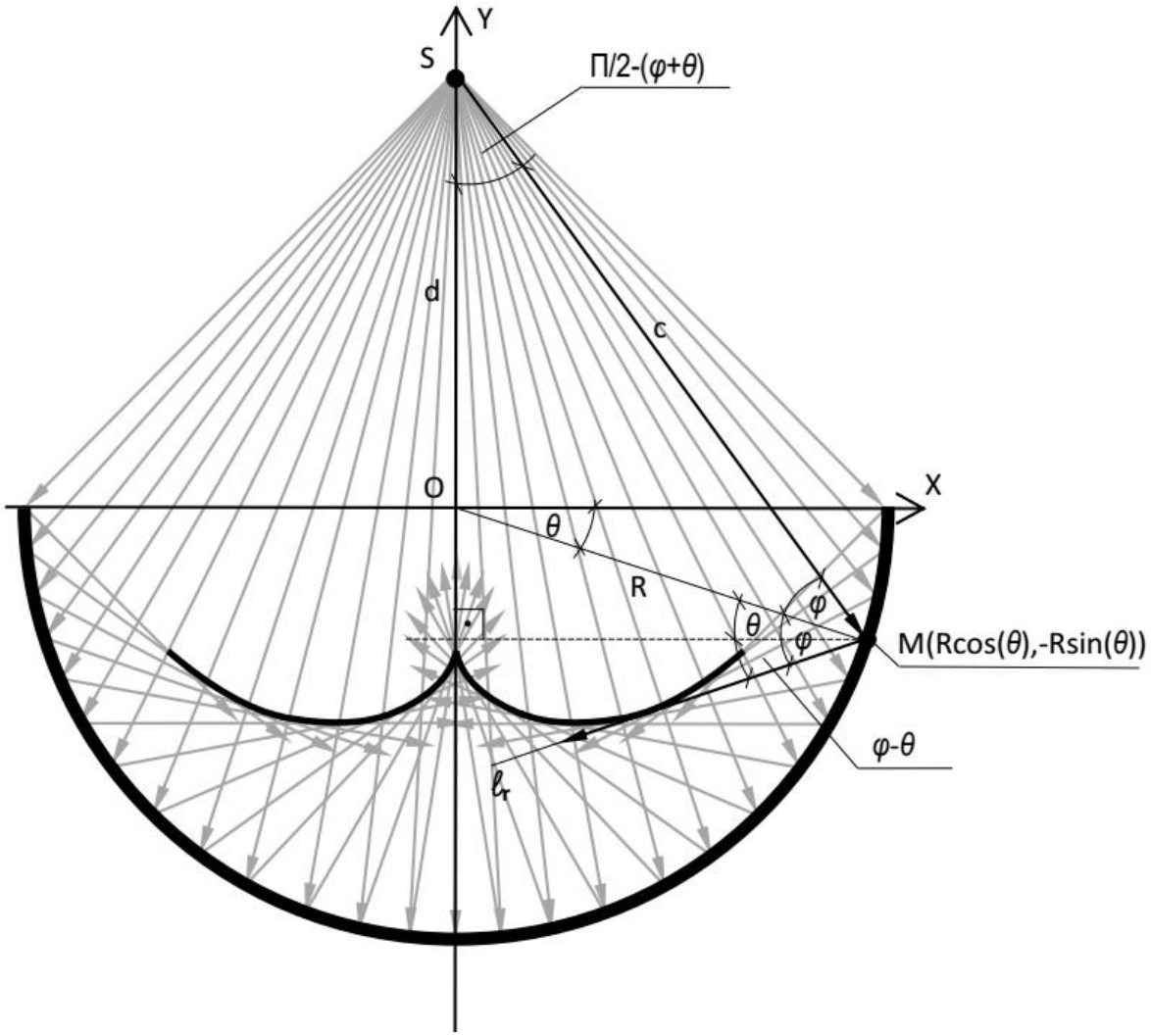

Fig. 1. A caustic formed by a concave hemispherical reflector, with the source of rays S on the axis of the reflector, outside the bowl of the reflector. S: the source of rays, R: the radius of the reflector, ℓ_r: the straight line describing the reflected ray.

The system of equations (15a)-(15c) is an analytic parametric description of the cross-section of the caustic, formed by a hemispherical or semicylindrical concave reflector of the radius R, at a specific distance d from the reflector. The system of equations (15a)-(15c) applies to the source located on the axis of the reflector, either inside or outside its bowl (d<0 and d>0, respectively).

The graphic form of the solution of systems of equations (15a)-(15c) is shown in Fig. 2. An example of a caustic with a source of rays inside the reflector bowl (d<0), together with the corre-

sponding bundle of rays is shown in Fig. 3. 3D views of the caustics formed by the spherical and cylindrical concave reflector are shown in Fig. 4.

When the source of rays is a point in infinity, the divergent rays from Fig. 1 become parallel. A caustic is then described by the system of equations (16), resulting from the system (15a)-(15c) at d going to infinity (Appendix 2). The plot of Eq. (16) is shown in Fig. 2a, d=∞).

$$\begin{cases} x(\theta) = R\cos^3(\theta) \\ y(\theta) = \frac{R}{2}\left(2\sin^3(\theta) - 3\sin(\theta)\right) \end{cases} \qquad 0 \le \theta \le \Pi \tag{16}$$

The system of equations (16) describes also the nephroid, i.e. a curve drawn by a fixed point of a circle rolling outside another circle, with the ratio between their radii as 1:2 [12] (Fig. 5).

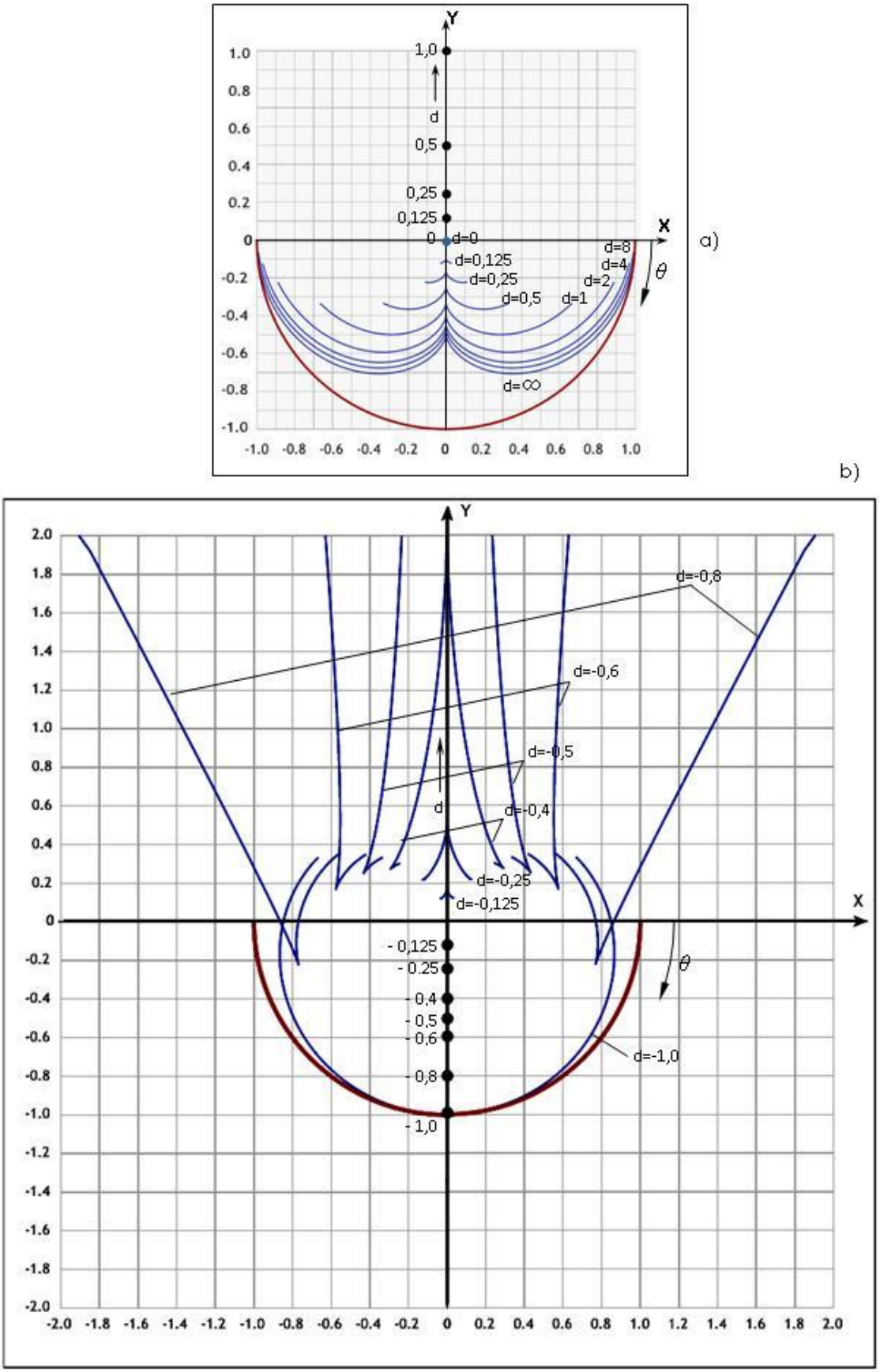

Fig. 2. The graphic form of the solution of systems of equations (15a)-(15c) and (16), for R=1 and the source located outside (a) and inside (b) the reflector bowl (d>0 and d<0, respectively.) The diagrams show the cross-sections of caustics (thin lines) created by a hemispherical or semicylindrical reflector (thick line). The reflector is described by the system of equations {x(θ)=cos(θ), y(θ)=-sin(θ)}. Plot by [13].

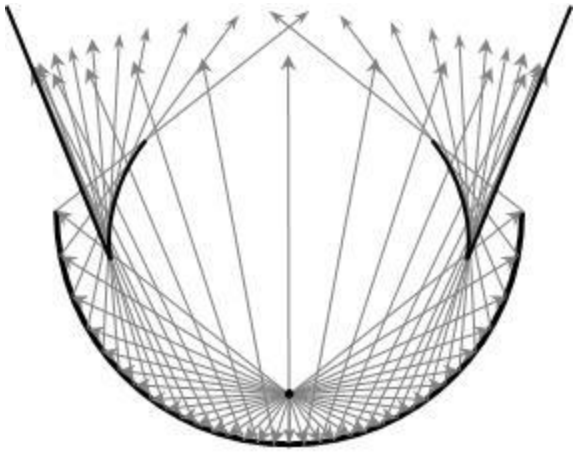

Fig. 3. An example of a caustic with a source of rays inside the reflector bowl with the radius R=1, together with the corresponding bundle of rays (compare Fig. 2b, d = -0.8m).

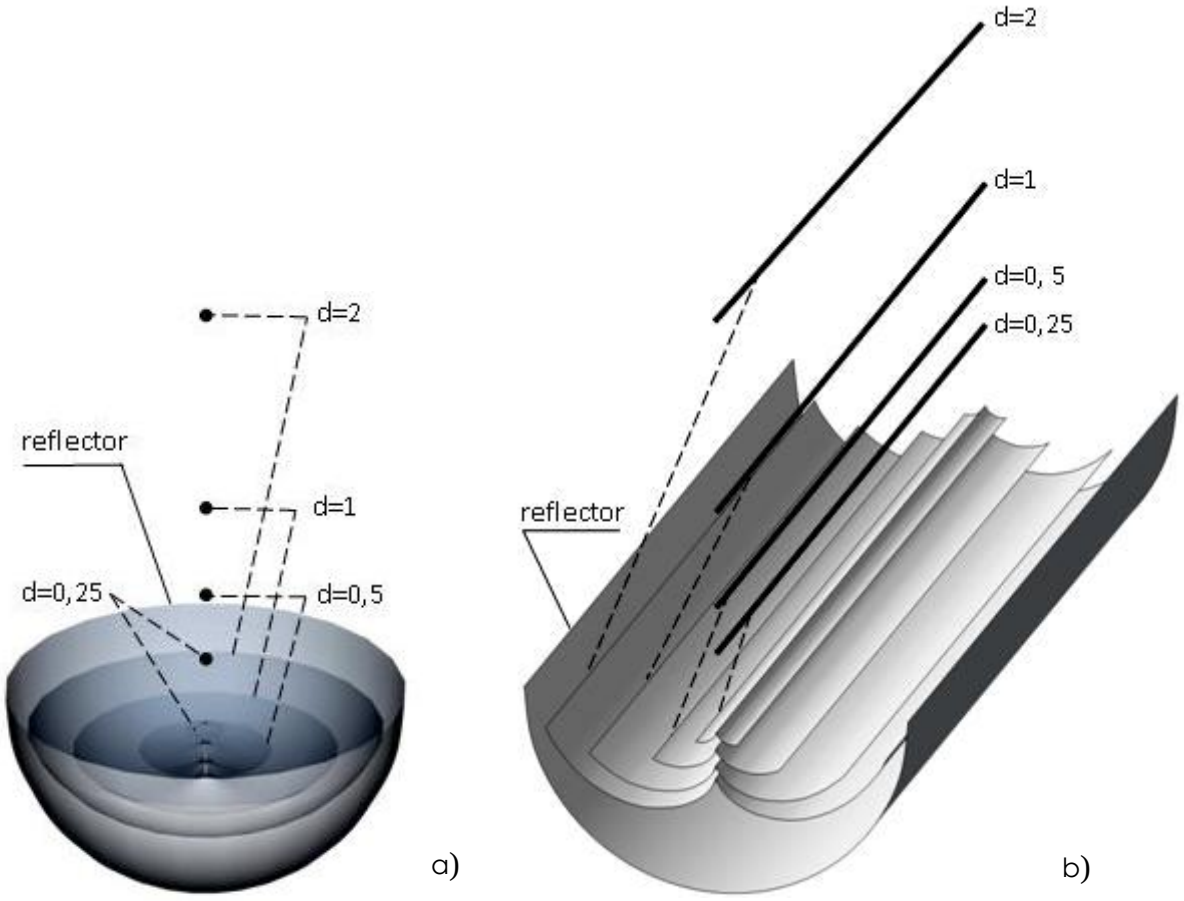

Fig. 4. 3D views of the caustics formed by the hemispherical a) and semicylindrical b) concave reflector with the radius R=1. The point-like a) and linear b) sources of rays are situated at a distance of d=0.25m, d=0.5m, d=1m, d=2m from the centre of the reflector.

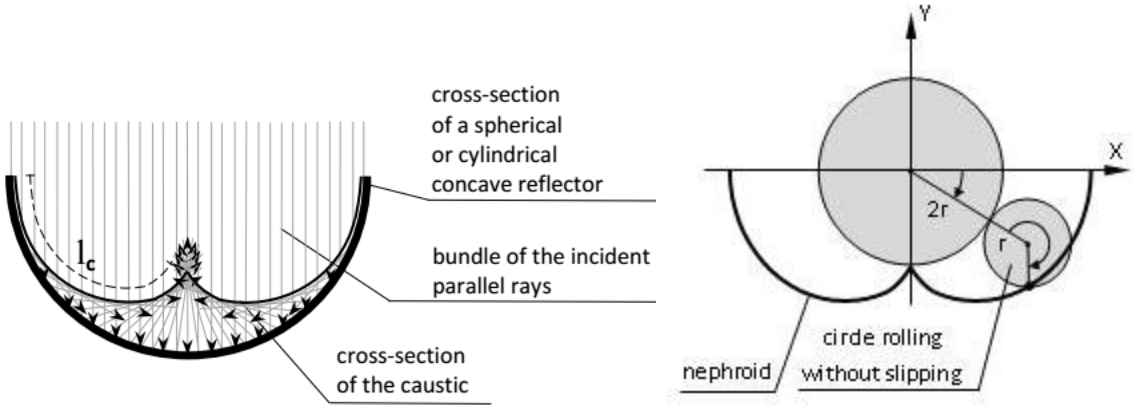

a) b)

Fig. 5. The caustic created by a parallel bundle of rays (a) and the nephroid (b).

Both curves are described by the system of equations (16).

l_C: half the length of the axial section of the caustic (refers to Eq.(29)).

Due to the spherical symmetry of the hemisphere and the axial symmetry of the semicylinder, placing of the source of rays outside the axis of the reflector is equivalent to the rotation of the axis by the angle α around the point (0,0) (Fig. 6, compare Fig. 2a for the case d=1). The formation of a caustic shown in Fig. 1 along with the Eqs. (15a)-(15c) and (16) still apply in the range of angle θ $\alpha \leq \theta \leq \Pi+\alpha$. The caustics calculated according to this convention are shown in Fig. 7. The above procedure does not apply to reflectors that do not have spherical symmetry, e.g. elliptic or parabolic.

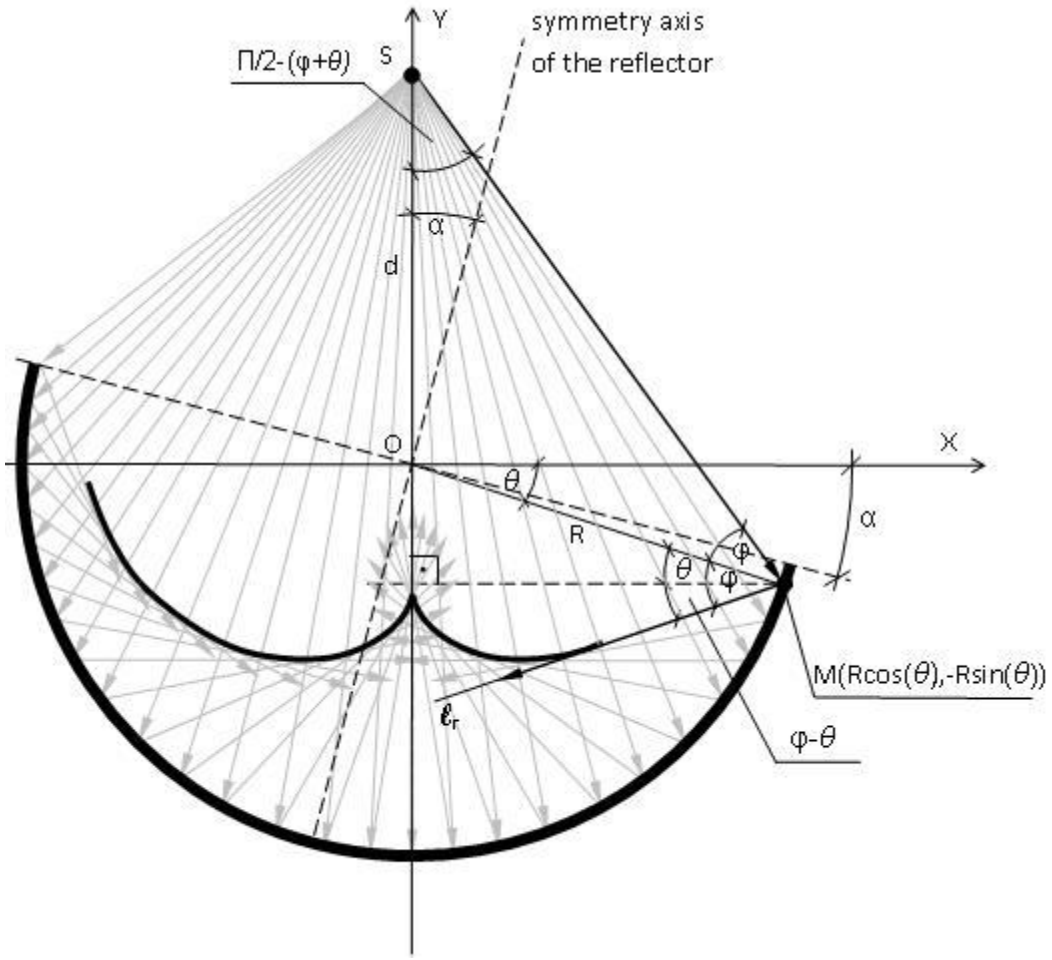

Fig. 6. A caustic formed by a concave hemispherical reflector with the radius R, for the source of rays S outside the axis of the reflector.

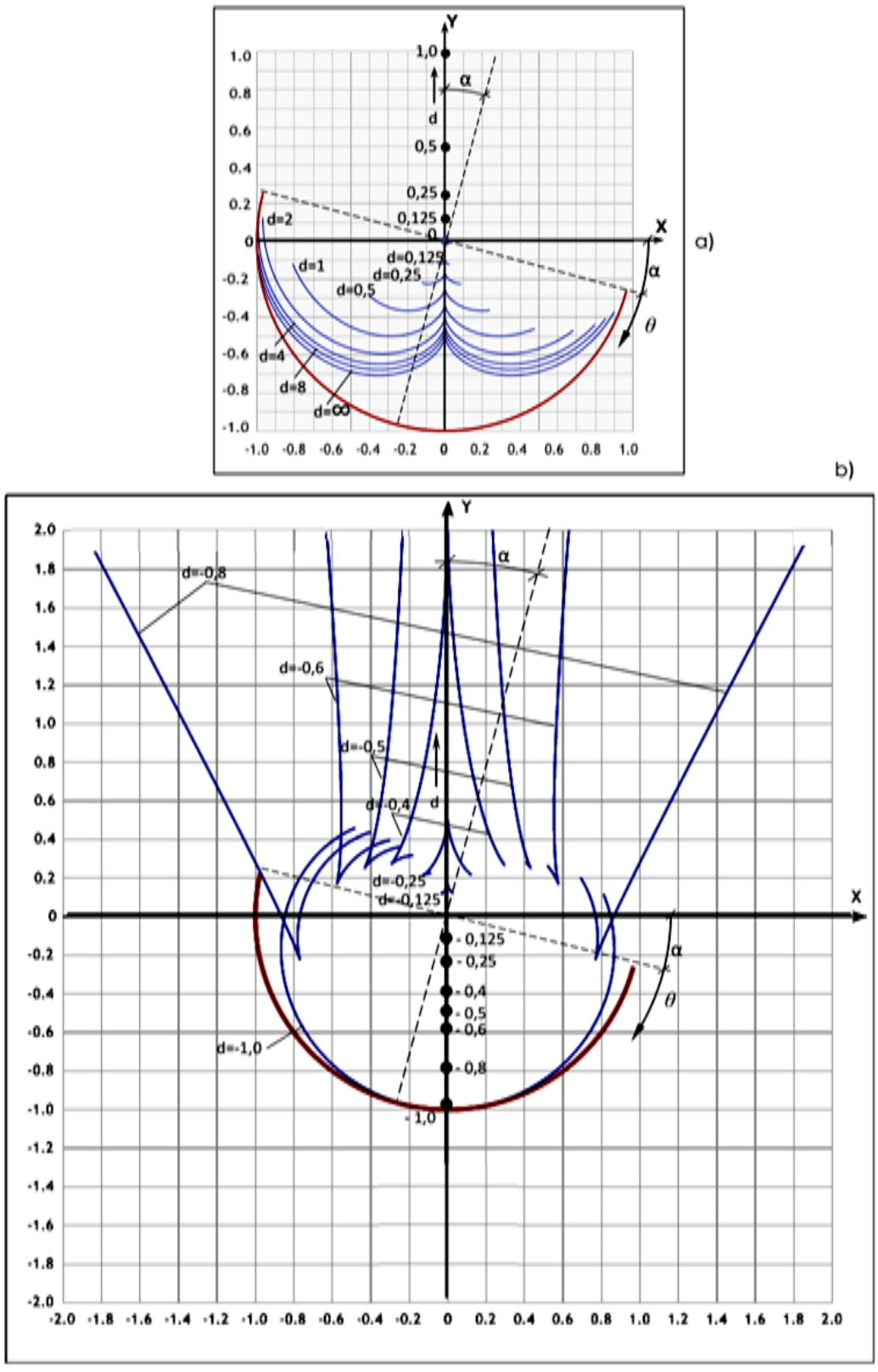

Fig. 7. The graphic form of the solutions of Eq. (15a)-(15c) and (16) for several positions of the source of rays located out of the axis of symmetry of the hemispherical reflector ($\alpha \leq \theta \leq \Pi + \alpha$).

3. Ray density over a caustic

Consider a bundle of parallel rays incident on a hemispherical concave reflector and look at two rings: dS on a surface of a reflector and dS_c on a caustic. (Fig. 8) [14]. All rays reflected from dS are tangent to dS_c, so the measure of the density of rays on dS_c is the ratio of the surfaces of these rings dS/dS_c

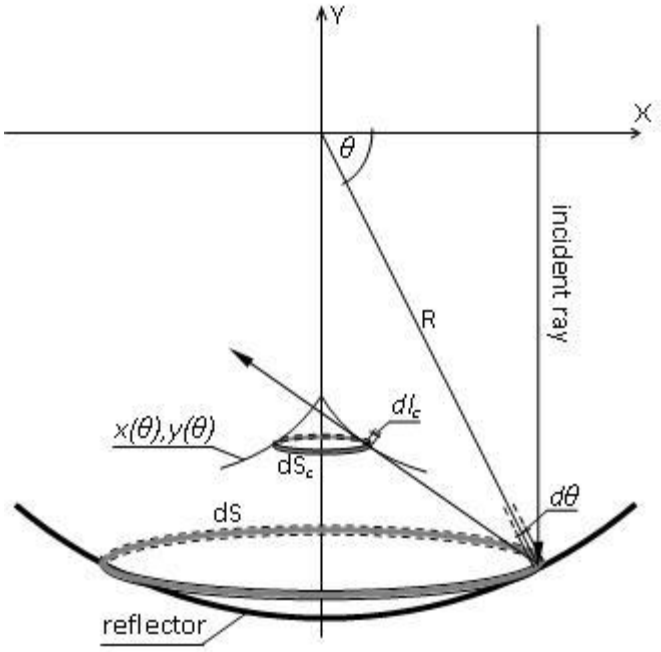

Fig. 8. The caustic formed by a bundle of parallel rays incident on a concave hemispherical reflector. R: radius of the reflector, dS, dS_c: the ring on the surface of a reflector and on the caustic, respectively, *x(θ),y(θ):* Cartesian coordinates of the caustic (see Eq. (16)), dl_c: the element of length along the axial cross-section of the caustic.

The length of the ring dS is $2\Pi R\cos(\theta)$ and its width, seen from the source of the rays at infinity, is $R\sin(\theta)d\theta$, so its dS is

$$dS = 2\Pi R^2 \cos(\theta) \sin(\theta)\, d\theta \tag{17}$$

Similarly, the length and the width of the ring dS_c are $2\Pi x(\theta)$ and dl_c, respectively, so

$$dS_c = 2\Pi\, x(\theta)\, dl_c \tag{18}$$

where $x(\theta)$ is part of the parametric equation of the caustic (see Eq. (16)) and dl_c is the element of length along an axial cross-section of a caustic

$$dl_c = \left[\left(\frac{dx(\theta)}{d(\theta)}\right)^2 + \left(\frac{dy(\theta)}{d(\theta)}\right)^2\right]^{1/2} d\theta \quad (19)$$

x(θ), y(θ) are Cartesian coordinates of a point on the caustic given by Eq. (16), so their derivatives over θ are

$$\begin{cases} \frac{dx}{d\theta} = -3R\cos^2(\theta)\sin(\theta) \\ \frac{dy}{d\theta} = 3R\sin^2(\theta)\cos(\theta) - \frac{3}{2}R\cos(\theta) \end{cases} \quad (20)$$

so

$$\left(\frac{dx(\theta)}{d(\theta)}\right)^2 + \left(\frac{dy(\theta)}{d(\theta)}\right)^2 = \left(\frac{3}{2}R\cos(\theta)\right)^2\left[(-2\sin(\theta)\cos(\theta))^2 + (2\sin^2(\theta)-1)^2\right] =$$
$$\left(\frac{3}{2}R\cos(\theta)\right)^2\left[\sin^2(2\theta) + (2\sin^2(\theta) - \sin^2(\theta) - \cos^2(\theta))^2\right] = \left(\frac{3}{2}R\cos(\theta)\right)^2\left[\sin^2(2\theta) + \cos^2(2\theta)\right] = \left(\frac{3}{2}R\cos(\theta)\right)^2 \quad (21)$$

Substituting Eq. (21) to Eq. (19) yields

$$dl_c = \frac{3}{2}R\cos(\theta)d\theta \quad (22)$$

so

$$dS_c = 2\Pi x(\theta)\mathrm{d}l_c = 3\Pi R^2\cos^4(\theta)\, d\theta \quad (23)$$

The density of rays *C(θ)*, which represents the focusing effect of the caustic, over the ring dS_c is then

$$C(\theta) = \frac{dS}{dS_c} = \frac{2\sin(\theta)}{3|\cos^3(\theta)|} \quad (24)$$

Denote the density of the rays incident on the reflector per a unit of time as I_o [W/m^2] and the absorption coefficient of the reflector as α, 0≤α≤1, where α=0 and α=1 relate to a total reflection and total absorption, respectively. Using the analogy between geometric optics and geometric acoustics, we have then

$$I_c(\theta) = I_o(1-\alpha)\, C(\theta) = I_o(1-\alpha)\frac{2\sin(\theta)}{3|\cos^3(\theta)|} \quad (25)$$

where $I_c(\theta)$ is a density of energy on the caustic per unit of time, which in the area of acoustics can be interpreted as a sound intensity [W/m^2]. According to Eq. (25), $I_c(\theta)$ is infinite at θ=Π/2 (see Fig. 9), since an area of the ring dS_c goes to zero at the cusp of the caustic, i.e. at vertical incidence, and zero at

$\theta=0$ and $\theta=\Pi$ where the incident rays are tangent to the reflector. The resultant sound intensity $I_{c,res}(\theta)$ is the sum of sound intensity over the caustic and the sound intensity of the incident rays

$$I_{c,res}(\theta) = \mathrm{I_o} + \mathrm{I_o}(1-\alpha)\frac{2\sin(\theta)}{3\,|\cos^3(\theta)|} = \mathrm{I_o}\left(1+(1-\alpha)\frac{2\sin(\theta)}{3\,|\cos^3(\theta)|}\right) \tag{26}$$

Taking $\mathrm{I_o}$ as the reference sound intensity, the resultant sound level over the caustic is $L_{c,res}(\theta)$ (Fig. 9)

$$L_{c,res}(\theta) = 10\log\frac{I_{c,res}(\theta)}{\mathrm{I_o}} = 10\log\left(1+(1-\alpha)\frac{2\sin(\theta)}{3\,|\cos^3(\theta)|}\right) \quad \text{[dB]} \tag{27}$$

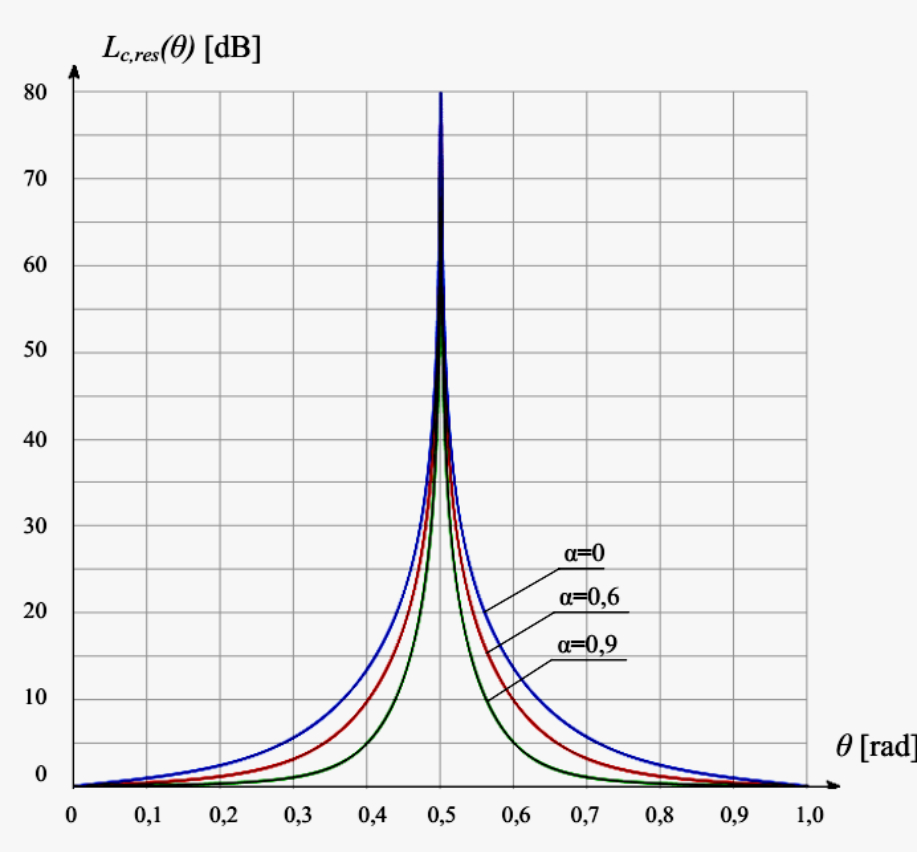

Fig. 9. Resultant sound level $L_{c,res}(\theta)$ [dB] over the caustic for the bundle of parallel rays incident on a hemispherical reflector. α: absorption coefficient of the reflector.

Multiplying the sound intensity $I_c(\theta)$ [W/m^2] by the area of ring dS_c [m^2] (Eqs.(25) and (18), respectively) yields the differential sound power $dP_c(\theta)$ [W], distributed over the caustic on the ring of the width dl_c (Eq. (28)

$$dP_c(\theta)= I_c(\theta)\, 2\Pi x(\theta) dl_c = I_o(1-\alpha)\frac{4}{3}\Pi R \sin(\theta) dl_c \tag{28}$$

As the power of incident rays is finite, sound power on the caustic P_c also remains finite, including the cusp of the caustic. At α=0, the total power over the caustic is equal to the power of bundle of rays incident on a reflector, as expected (Eq. (29)),

$$P_c = \int_0^{l_c} dP_c(\theta) dl_c = \int_0^{\Pi/2} I_o \frac{4}{3}\Pi R \sin(\theta)\frac{3}{2} R\cos(\theta) d\theta = I_o \Pi R^2 \int_0^{\Pi/2} \sin(2\theta) d\theta = I_o \Pi R^2 \tag{29}$$

where l_c is half the length of the axial section of the caustic (see Fig. 5a).

4. Impact of wave effects on a caustic

After the geometrical approach presented in Sections 3 and 4, in this chapter, the impact of interference and diffraction of waves on a caustic is estimated. First, the effect of the overlap of the wave incident on the mirror on the wave which creates a caustic is described. This phenomenon has been analyzed with reference to the harmonic signal, but in the rooms, it occurs in a wide frequency range, which leads to blurring of the caustic shape. Then the contribution of diffraction in the deformation of a caustic is analyzed.

Consider a flat acoustic wave incident on the hemispherical reflector. If the wavelength λ is much smaller than the diameter of the reflector D, the principles of geometric acoustics apply [15], [16]. Later in this chapter, the case of λ/D = 0,035 is considered, which makes it possible to take the shape of a caustic as in Fig. 5a and the directions of interfering waves as in Fig. 10. Assume that at the moment t=0 the wavefront incident on the reflector lies in the plane y=0. In its further course, it interferes with the reflected wave. This phenomenon occurs throughout the entire area in which the reflected wave is present, both inside and outside the reflector's bowl. The following analysis applies only to the cross-section of caustics shown in Fig. 10.

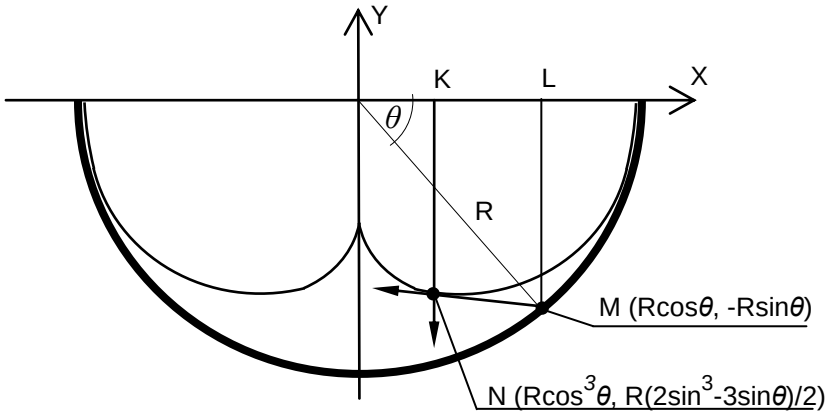

Fig. 10. Directions of the incident and reflected waves, KN and LMN, respectively, which interfere over the cross-section of the caustics. R: the radius of the reflector.

The distances S_{KN} i S_{LMN} travelled by the incident and reflected waves are (see Eq.16)

$$S_{KN} = \frac{R}{2}\left|2\sin^3\theta - 3\sin\theta\right| = \frac{R}{2}\left(3\sin\theta - 2\sin^3\theta\right), \qquad 0 \le \theta \le \Pi \tag{30}$$

$$S_{LMN} = S_{LM} + S_{MN} = R\sin\theta + \sqrt{\left(R\cos\theta - R\cos^3\theta\right)^2 + \left(-R\sin\theta - \left(\frac{R}{2}\left(2\sin^3\theta - 3\sin\theta\right)\right)\right)^2} =$$

$$R\sin\theta + \sqrt{\left(\frac{R}{2}\sin\theta\sin 2\theta\right)^2 + \left(\frac{R}{2}\sin\theta\cos 2\theta\right)^2} = R\sin\theta + \frac{R}{2}\sin\theta\sqrt{(\sin 2\theta)^2 + (\cos 2\theta)^2} = \frac{3}{2}R\sin\theta, \qquad 0 \le \theta \le \Pi \tag{31}$$

Note that y coordinates of the points N and M are negative because these points are on the negative part of the Y-axis. As S_{KN} and S_{LMN} must be positive, Eqs. (30) and (31) contain the absolute values of the expressions $|R(2\sin^3\theta - 3\sin\theta)/2|$ and $|-R\sin\theta|$ which are $R(3\sin\theta - 2\sin^3\theta)/2$ and $R\sin\theta$, respectively.

$I_c(\theta)$ is interpreted as the sound intensity on the caustic (see Eq. (25)). As sound intensity I is proportional to a squared sound pressure p

$$I = p^2/2\rho c \tag{32}$$

where ρ: the density of the medium, c: the speed of sound in the medium (in the air $\rho c = 415[Ns/m^3]$), the amplitude of the sound pressure $|p_c(\theta)|$ of the wave condensed on the caustic is

$$|p_c(\theta)| = \sqrt{\frac{I_c(\theta)}{2\rho c}} = \sqrt{\frac{I_o}{2\rho c}} \sqrt{\frac{2(1-\alpha)\sin(\theta)}{3|\cos^3(\theta)|}} \tag{33}$$

Taking I_o as the intensity of the sound incident on the reflector (see Eq. (25)), sound pressure $p_i(t)$ of the incident wave is

$$p_i(t) = \sqrt{\frac{I_o}{2\rho c}} \sin \varpi t \tag{34}$$

where $\omega=2\Pi f$, f: frequency [Hz]. Assuming lossless wave propagation, after travelling the distance S_{KN} the sound pressure is

$$p_{KN}(t) = \sqrt{\frac{I_o}{2\rho c}} \sin \varpi (t + \Delta t_1), \qquad \Delta t_1 = S_{KN}/c \tag{35), (36}$$

and after travelling the distance S_{LMN} and condensation on the caustic according to Eq. (33)

$$p_{LMN}(t,\theta) = \sqrt{\frac{I_o}{2\rho c}} \sqrt{\frac{2(1-\alpha)\sin(\theta)}{3|\cos^3(\theta)|}} \sin \varpi (t + \Delta t_2), \qquad \Delta t_2 = S_{LMN}/c \tag{37), (38}$$

Resultant sound pressure on the caustic $p_{c,res}(t,\theta)$ [Pa] is then

$$p_{c,res}(t,\theta) = \sqrt{\frac{I_o}{2\rho c}} \left(\sin \varpi (t + \Delta t1) + \sqrt{\frac{2(1-\alpha)\sin(\theta)}{3|\cos^3(\theta)|}} \sin \varpi (t + \Delta t_2) \right) \tag{39}$$

The difference of the phase $\Delta t1$-$\Delta t2$ between the components of Eq. (39) varies with θ (Appendix 3, line A3.8). This causes $p_{c,res}(t,\theta)$ to fluctuate on the caustic over time. Fluctuations are in the form of amplitude modulation, the maximum range of which results from Eq. (40) (Appendix 3)

$$\frac{d}{dt} p_{c,res}(t) = 0 \tag{40}$$

what gives

$$t = \frac{1}{\varpi} \operatorname{arctg}(q) - \Delta t_1 \tag{41}$$

where

$$q = \frac{\sqrt{\frac{3|\cos^3\theta|}{2(1-\alpha)\sin\theta}} + \cos\left(\varpi \frac{R \sin^3\theta}{c}\right)}{\sin\left(\varpi \frac{R \sin^3\theta}{c}\right)} \tag{42}$$

Substitution t to Eq.(39) yields the maximum range of amplitude modulation $p_{c,res,Max}(\theta)$ [Pa]

$$p_{c,res,Max}(\theta) = \sqrt{\frac{I_o}{2\rho c}} \left[\sin(\operatorname{arctg}(q)) + \sqrt{\frac{2(1-\alpha)\sin(\theta)}{3|\cos^3(\theta)|}} \sin\left(\operatorname{arctg}(q) + \varpi \frac{R \sin^3\theta}{c}\right) \right] \tag{43}$$

The result of the interference of the wave incident on the mirror of a diameter D=2m with the reflected wave of a wavelength λ=0,07m line is shown in Fig. 11. The frequency of the wave f=4800 Hz refers to the example shown in the next chapter. At the intensity of the incident wave I_o=1 [W/m^2], the amplitude $\overline{p_i}$ of the sound pressure of the incident wave propagating in the air is (see Fig. 11, dashed line).

$$\overline{p_i} = \sqrt{I_o/(2\rho c)} = \sqrt{1/(2*415)} \cong 0{,}035 \text{ [Pa]} \tag{44}$$

The resultant sound pressure level on the caustic $SPL_{c,res}(\theta)$ re. 2x10^{-5} [Pa] is (Fig. 12)

$$SPL_{c,res}(\theta) = 20\log\left(p_{c,res,\max}(\theta)/(2*10^{-5})\right) \tag{45}$$

Taking the sound intensity of the incident wave I_o=1W/m^2, its sound pressure level SPL_i is

$$SPL_i = 20\log\left(\sqrt{1/(2*415)}/(2*10^{-5})\right) = 65\text{dB} \tag{46}$$

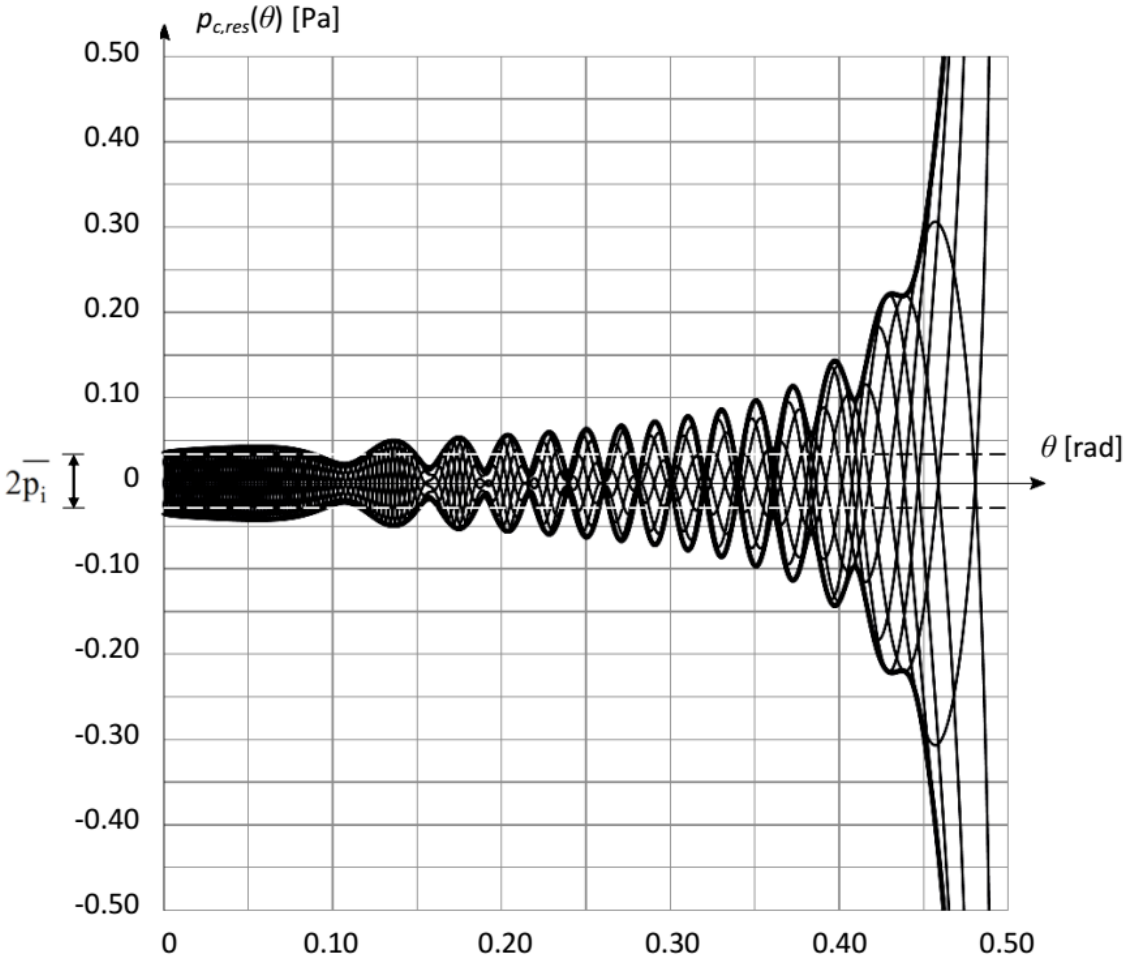

Fig. 11. The result of the interference of the plane wave of the frequency f=4800 Hz, incident on a hemispherical reflector, with the wave which forms the caustic. Sound pressure of the resultant wave $p_{c,res}(t,\theta)$ is shown with a thin line at the moments of time t = 0, T/8, ..., 7T/8, where T=1/f. Its maximum amplitude $p_{c,res,Max}(\theta)$ is shown with a thick line. R=1m, α=0, $\overline{p_i}$: the amplitude of sound pressure of the incident wave. Due to symmetry, the range $0 \le \theta \le \Pi/2$ is shown.

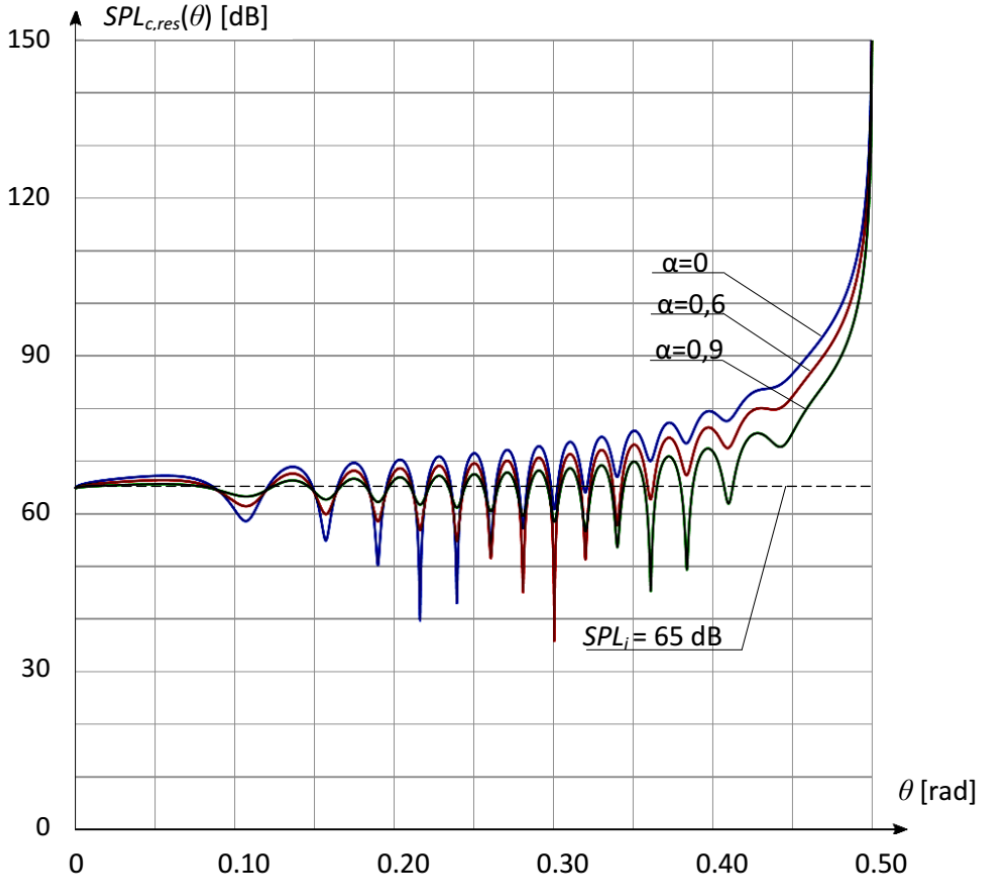

Fig. 12. Resultant sound pressure level $SPL_{c,res}(\theta)$ of the flat wave with the frequency f=4800 Hz incident on the hemispherical reflector with the diameter R=1m, interfering with the reflected wave on the caustic. SPL_i: sound pressure level of the incident wave. α: absorption coefficient of the reflector. Due to symmetry, the range $0 \le \theta \le \Pi/2$ is shown.

Regardless of the influence of interference on caustics described above, it is distorted due to the deflection of the wave at the edge of the mirror. In the context of optics, the relationship between the wavelength λ and the angle ξ of its deflection on the edge of the device of a circular aperture with radius R, e.g. a lens, a mirror or a hole in a screen, is given by the Rayleigh criterion [17]

$$\xi = 1{,}22\frac{\lambda}{R}[\text{rad}] \tag{47}$$

Eq. (47) is an empirical measure adopted for assessing the quarter-wave resolution in the imaging process of the objects distant from the lens or mirror. In the cases considered below, the caustics are inside the mirror bowl, and the wavelength of sound is several orders of magnitude larger than the wavelength of light. In this case, the Rayleigh criterion serves just as a rough estimation of the impact of diffraction on the effective shape of the caustic [10]. Fig. 13 shows the blur of the caustics formed by the reflection of the plane wave (see Fig. 5a) with a wavelength of 14 cm and 3.5 cm. The effect of wave diffraction increases with a wavelength, so the sound focusing area on the caustics expands as the frequency of the sound decreases.

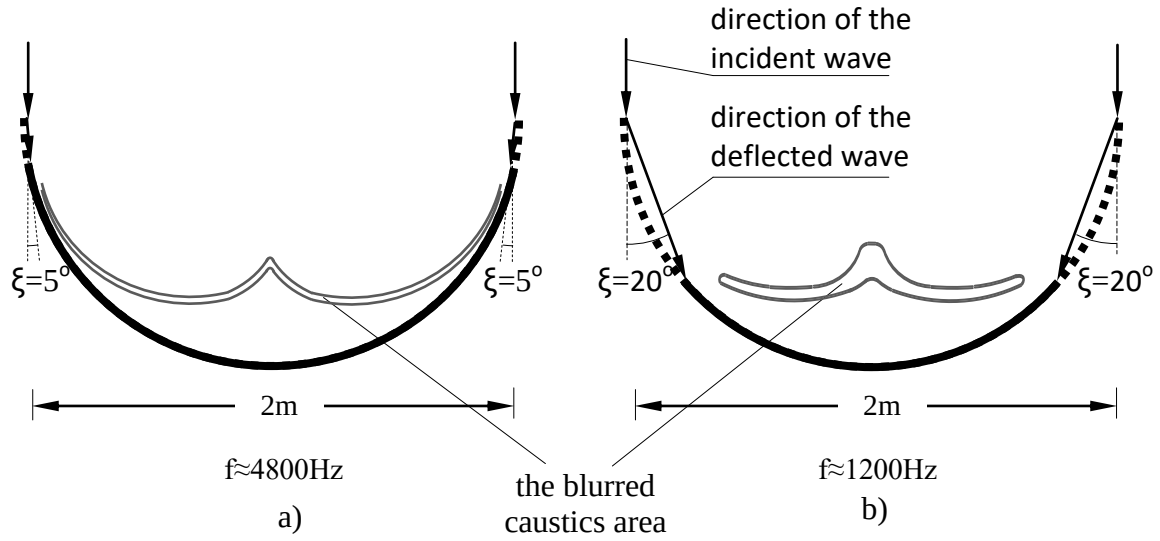

Fig. 13. A rough assessment of the λ/4 blur of a caustic using the Rayleigh criterion. The caustics are formed by the plane wave with a frequency of ca. 4800 Hz and 1200 Hz incident on a hemispherical reflector with a radius of R=1m (a and b, respectively). ξ: the angle of the wave deflection due to the Rayleigh criterion. The part of the reflector forming the caustic is marked with a thick solid line.

5. Caustics in architectural acoustics

The dominant form of acoustic phenomena in rooms are sequences of sound built-up and decay, which are the room response to speech and music. With such stimulation of the room with arched vaults and concave walls, an objective manifestation of sound concentration is the uneven distribution of the room acoustic parameters. It is superimposed by subjective impressions in the form of deformation of directional effects and distortions in the perception of the timbre of the sound [1].

In a room, the geometrically ordered image of caustics shown in Fig. 2 and 4 may blur. The main reason for this is the presence of diffuse sound, which at a high intensity of reverberant sound blurs and partially masks the caustics. Wave effects in the form of interference and a quarter-wave image resolution due to the Rayleigh effect interact in a similar way. The broadband nature of the sounds in the room increases the impact of these wave effects. Therefore, at high intensity of these factors, it may happen that only the caustic cusp in the form of a sound focus is found, and the rest of the caustic is seemingly absent.

Fig. 14a shows the Assembly Hall of Poznań University, Poland. This form of interior is often found in concert halls and theatres of the 19th century and is considered to be acoustically unfavorable due to the concave vault [1]. In order to avoid the effect of focusing the sound perceived by listeners, an appropriate ratio between the room height h and the radius of the concave vault r should be kept. E.g. the recommendation for the room with the shape shown in Fig. 14 is $r \leq h/2$ [19]. Fortunately, this room is known for its good acoustics as the venue of the Henryk Wieniawski International Violin Competition taking place for almost 80 years. The stage with the sound sources is located outside the reflector bowl that refers to the caustic system shown in Fig. 2a. Fig. 14b shows the 3D image of the caustic, corresponding to the case $d \approx R$, where R is the radius of the semicylindrical vault and d is the distance between the sound source and the center of the vault. The presented example shows that when the area of sound concentration is significantly above the audience's presence area, it is possible to reconcile acoustic requirements with the architectural expression of a historic room.

Fig. 15 shows objects in which, due to their historical value, the architectural priority prevails over the acoustic one, and the acoustic effects, obviously unfavorable in concert and theatre halls, become the acoustic specificity of this place.

The effect of sound concentration can also occur in the open air, produced by large objects with a concave form, e.g. concert shells, frontages of buildings, etc. Fig. 16 a) shows the 1933 concert shell in Gdynia (Poland) in the form of a 1/4 sphere. Fig. 16 b) presents the horizontal cross-sections of caustics, determined according to the rules of geometric optics. A rough assessment of the blur of the caustic is shown in Fig. 16 c) and d). The presented example shows that oval concert shells cover the audience with sound unevenly, with areas of sound concentration depending on the location of the source.

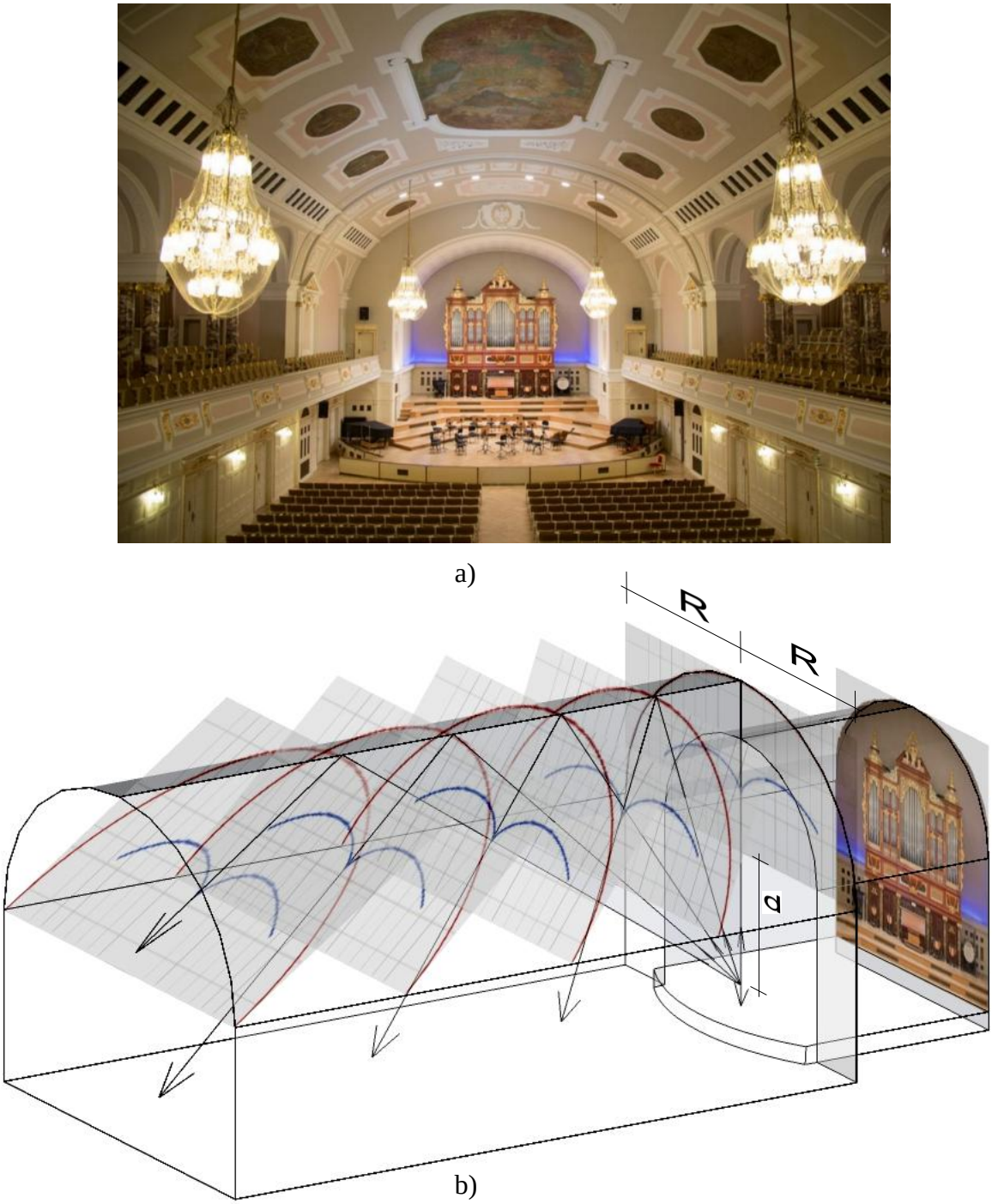

Fig. 14. a) Assembly Hall of Poznań University. This neo-renaissance building was erected according to the design of Edward Fürstenau in 1905-1910, photo courtesy of Poznań Film Commission [18].

b) Cross-sections of the 3D caustic, corresponding to the case d=1 from Figs. 2a and 4b.

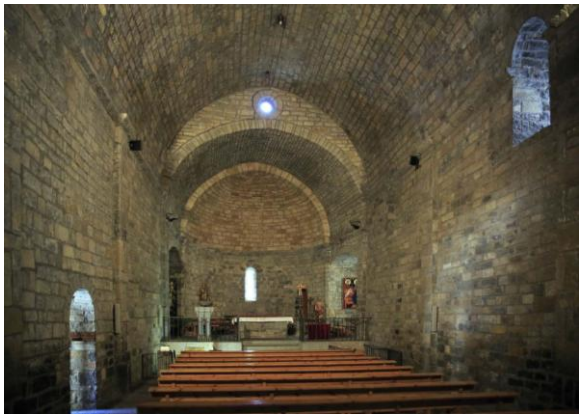

a)

b)

c)

Fig. 15. a) The barrel vault in the church of Santa Maria in Aisna, Spain (11th/12th century) [20].

b) The barrel vault in Abbaye de Boscodon, France (12th century). Photo by Morburre CC BY-SA 3.0 [21].

c) Church of Santa_Maria_Assunta_di_Torcello, Venice, Italy (11th century).

Photo by Remi Mathis CC BY-SA 3.0 [22].

a)

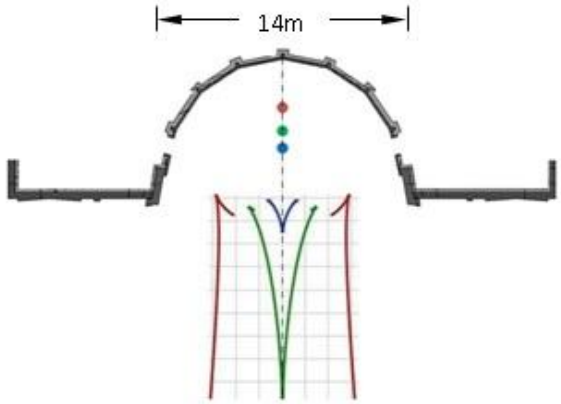

b)

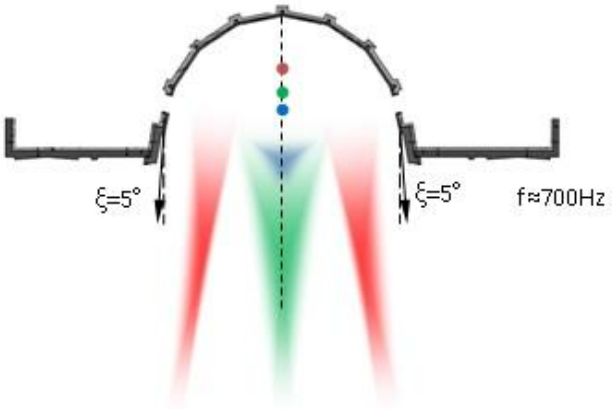

c)

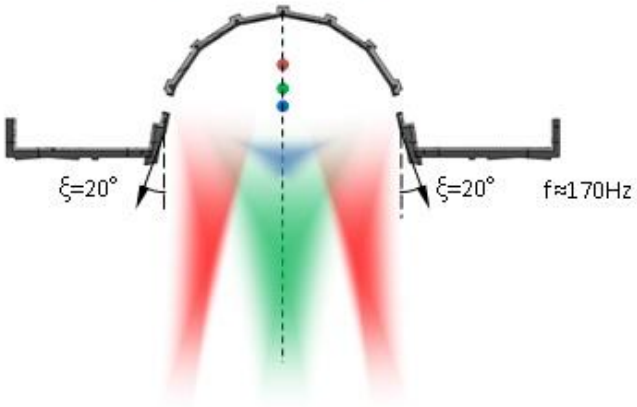

d)

Fig. 16. a) The outdoor concert shell in Gdynia, Poland, photo courtesy of Karol Stańczak [23].
b) The horizontal cross-sections of the caustics, corresponding to three positions of the sound source from Figure 2b: d = -0,25R (blue), d = -0,4R (green), d = -0,6R (red), R: the radius of the shell, R=7m. c) and d) A rough assessment of the λ/4 blur of the caustics due to the Rayleigh criterion. The caustics are formed by the wave with a frequency of ca. 700 Hz and 170 Hz, respectively. ξ: the angle of the wave deflection related to the Rayleigh criterion. (For interpretation of the references to colour in this figure legend, the reader is referred to the web version of this article.)

6. Concluding remarks

In rooms with concave architectural elements, the area of sound concentration usually takes a form in which it is difficult to find a geometrically ordered shape of a caustic. For this reason, the concept of caustics is almost unknown in the field of architectural acoustics. The article explains the mechanism of the caustic's blur. It is attributed to interference and diffraction, whose impact on caustics is further intensified due to the broadband nature of the sound in the rooms. When one also takes into account momentary changes in the volume of sound, which are a natural feature of music and speech, caustics is reduced to its singularity. Its observed form is a point focus of sound, while the rest of the caustics is blurred to such an extent that it becomes invisible.

As a physical phenomenon in the field of acoustics, caustics are usually considered blurred, i.e. secondary form of the sound condensation. However, the mathematical description of caustics shows an inverse interpretation, i.e. caustics should be treated as the primary form of sound condensation, whose singularity is the focus. The purpose of this article is to present this point of view. In the article, an analytic formula for the cross-section of a caustic is derived, with the source of rays located at a specific distance from the reflector. Then the ray density distribution over a caustic is evaluated. Finally, the impact of wave effects, like interference and roughly assessed diffraction of waves, on a caustic blur is analyzed. As a physical representation of caustics, its shape indoors and outdoors in selected architectural objects is presented.

APPENDIX 1

Derivation of the system of equations {x(θ), y(θ)} (Eqs. (15a)-(15c) - lines A1.18, A1.19)

$$y(x,\theta,\varphi) = tg(\varphi-\theta)(x-R\cos(\theta)) - R\sin(\theta)$$

$$\frac{dy}{d\varphi} = \frac{\delta y}{\delta\varphi} + \frac{\delta y}{\delta\theta}\times\frac{\delta\theta}{\delta\varphi} = (x - R\cos(\theta))\frac{1}{\cos^2(\varphi - \theta)}$$

$$+\left(\frac{\delta tg(\varphi - \theta)}{\delta\theta}(x - R\cos(\theta)) + tg(\varphi - \theta)\frac{\delta(x - R\cos(\theta))}{\delta\theta} + \frac{\delta(-R\sin(\theta))}{\delta\theta}\right)\times\frac{\delta}{\delta\varphi}\left(\arccos(\frac{R}{d}\sin(\varphi)) - \varphi\right) = \tag{A1.1}$$

$$\frac{x - R\cos(\theta)}{\cos^2(\varphi - \theta)} + \left(\frac{-(x - R\cos(\theta))}{\cos^2(\varphi - \theta)} + tg(\varphi - \theta)R\sin(\theta) - R\cos(\theta)\right)\times\left(\frac{-1}{\sqrt{1 - (\frac{R}{d}\sin(\varphi))^2}}\frac{R}{d}\cos(\varphi) - 1\right) = \tag{A1.2}$$

$$\frac{x - R\cos(\theta)}{\cos^2(\varphi - \theta)} - \frac{(x - R\cos(\theta))}{\cos^2(\varphi - \theta)}\times\left(\frac{-R\cos(\varphi)}{\sqrt{d^2 - R^2\sin^2(\varphi)}} - 1\right) + R\left(tg(\varphi - \theta)\sin(\theta) - \cos(\theta)\right)\times\left(\frac{-R\cos(\varphi)}{\sqrt{d^2 - R^2\sin^2(\varphi)}} - 1\right) = \tag{A1.3}$$

$$\frac{x - R\cos(\theta)}{\cos^2(\varphi - \theta)}\left(1 + \frac{R\cos(\varphi)}{\sqrt{d^2 - R^2\sin^2(\varphi)}} + 1\right) - R\left(tg(\varphi - \theta)\sin(\theta) - \cos(\theta)\right)\times\left(\frac{R\cos(\varphi)}{\sqrt{d^2 - R^2\sin^2(\varphi)}} + 1\right) = 0 \tag{A1.4}$$

Extracting x(θ) from Eq. (A1.4):

$$x(\theta) = R\left(tg(\varphi - \theta)\sin(\theta) - \cos(\theta)\right)\times\cos^2(\varphi - \theta)\times\frac{\sqrt{d^2 - R^2\sin^2(\varphi)} + R\cos(\varphi)}{2\sqrt{d^2 - R^2\sin^2(\varphi)} + R\cos(\varphi)} + R\cos(\theta) \tag{A1.5}$$

To be continued in line (A1.14) after eliminating the φ variable.

Let's make substitutions - lines (A1.6) to (A1.9):

$$\Gamma(\theta) = \varphi - \theta = \arcsin\left(\frac{d\cos(\theta)}{\sqrt{R^2 + d^2 + 2Rd\sin(\theta)}}\right) - \theta \tag{A1.6}$$

$$A(\theta) = R\left(tg(\Gamma(\theta))\sin(\theta) - \cos(\theta)\right) \times \cos^2(\Gamma(\theta)) \tag{A1.7}$$

$$\sin(\varphi) = \frac{d\cos(\theta)}{\sqrt{R^2 + d^2 + 2Rd\sin(\theta)}} \tag{A1.8}$$

$$\cos(\varphi) = \sqrt{1 - \sin^2(\theta)} = \sqrt{1 - \frac{d^2\cos^2(\theta)}{R^2 + d^2 + 2Rd\sin(\theta)}} = \sqrt{\frac{R^2 + d^2\left(1 - \cos^2(\theta)\right) + 2Rd\sin(\theta)}{R^2 + d^2 + 2Rd\sin(\theta)}} = \tag{A1.9) - (A.1.11}$$

$$= \sqrt{\frac{(R + d\sin(\theta))^2}{R^2 + d^2 + 2Rd\sin(\theta)}} = \frac{R + d\sin(\theta)}{\sqrt{R^2 + d^2 + 2Rd\sin(\theta)}} \tag{A1.12), (A.1.13}$$

Continuation of line (A1.5):

$$x(\theta) = A(\theta) \times \frac{\sqrt{d^2 - R^2\frac{d^2\cos^2(\theta)}{R^2 + d^2 + 2Rd\sin(\theta)}} + R\frac{R + d\sin(\theta)}{\sqrt{R^2 + d^2 + 2Rd\sin(\theta)}}}{2\sqrt{d^2 - R^2\frac{d^2\cos^2(\theta)}{R^2 + d^2 + 2Rd\sin(\theta)}} + R\frac{R + d\sin(\theta)}{\sqrt{R^2 + d^2 + 2Rd\sin(\theta)}}} + R\cos(\theta) = \tag{A1.14}$$

$$A(\theta) \times \frac{d\sqrt{R^2\sin^2(\theta) + d^2 + 2Rd\sin(\theta)} + R(R + d\sin(\theta))}{2d\sqrt{R^2\sin^2(\theta) + d^2 + 2Rd\sin(\theta)} + R(R + d\sin(\theta))} + R\cos(\theta) = \tag{A1.15}$$

$$A(\theta) \times \frac{d\sqrt{(R\sin(\theta) + d)^2} + R(R + d\sin(\theta))}{2d\sqrt{(R\sin(\theta) + d)^2} + R(R + d\sin(\theta))} + R\cos(\theta) = \tag{A1.16}$$

$$A(\theta) \times \frac{Rd\sin(\theta) + d^2 + R^2 + Rd\sin(\theta)}{2Rd\sin(\theta) + 2d^2 + R^2 + Rd\sin(\theta)} + R\cos(\theta) \tag{A1.17}$$

Finally

$$\begin{cases} x(\theta) = A(\theta) \times \dfrac{R^2 + d^2 + 2Rd\sin(\theta)}{R^2 + 2d^2 + 3Rd\sin(\theta)} + R\cos(\theta) & \text{(A1.18)} \\ y(\theta) = tg(\Gamma(\theta))(x - R\cos(\theta)) - R\sin(\theta) & \text{(A1.19)} \end{cases}$$

APPENDIX 2

Derivation of Eq. (16) for a caustic with an infinitely distant source

(lines A2.11, A2.19)

$$\lim_{d\to\infty} x(\theta) = R\left(-\cos(\theta) + \sin(\theta) \times tg\left((\arcsin\left(\lim_{d\to\infty} \left(\frac{d\cos(\theta)}{\sqrt{R^2 + d^2 + 2Rd\sin(\theta)}} \right) \right) - \theta) \right) \right)$$

$$\times \cos^2\left(\arcsin\left(\lim_{d\to\infty} \left(\frac{d\cos(\theta)}{\sqrt{R^2 + d^2 + 2Rd\sin(\theta)}} \right) \right) - \theta \right) \times \lim_{d\to\theta} \left(\frac{R^2 + d^2 + 2Rd\sin(\theta)}{R^2 + 2d^2 + 3Rd\sin(\theta)} \right) + R\cos(\theta) = \quad \text{(A2.1)}$$

To be continued in line (A2.4).

$$\lim_{d\to\infty} \left(\frac{d\cos(\theta)}{\sqrt{R^2 + d^2 + 2Rd\sin(\theta)}} \right) = \lim_{d\to\infty} \left(\frac{d\cos(\theta)}{d\sqrt{\frac{R^2}{d^2} + \frac{d^2}{d^2} + \frac{2Rd\sin(\theta)}{d^2}}} \right) = \frac{\cos(\theta)}{\sqrt{0+1+0}} = \cos(\theta) \quad \text{(A2.2)}$$

$$\lim_{d\to\theta} \left(\frac{R^2 + d^2 + 2Rd\sin(\theta)}{R^2 + 2d^2 + 3Rd\sin(\theta)} \right) = \lim_{d\to\theta} \left(\frac{d^2\left(\frac{R^2}{d^2} + \frac{d^2}{d^2} + \frac{2Rd\sin(\theta)}{d^2} \right)}{d^2\left(\frac{R^2}{d^2} + \frac{2d^2}{d^2} + \frac{3Rd\sin(\theta)}{d^2} \right)} \right) = \frac{0+1+0}{0+2+0} = \frac{1}{2} \quad \text{(A2.3)}$$

$$R(-\cos(\theta) + \sin(\theta) \times tg(\arcsin(\cos(\theta)) - \theta)) \times \cos^2\left(\arcsin(\cos(\theta))\right) - \theta) \times \frac{1}{2} + R\cos(\theta) = \quad \text{(A2.4)}$$

$$R\left(-\cos(\theta) + \sin(\theta) \times tg(\arcsin\left(\sin(\frac{\Pi}{2} - \theta) \right) - \theta) \right) \times \cos^2\left(\arcsin\left(\sin(\frac{\Pi}{2} - \theta) \right) - \theta \right) \times \frac{1}{2} + R\cos(\theta) = \quad \text{(A2.5)}$$

$$R\left(-\cos(\theta) + \sin(\theta) \times \frac{1}{tg(2\theta)} \right) \times \cos^2(\frac{\Pi}{2} - 2\theta) \times \frac{1}{2} + R\cos(\theta) = R\left(-\cos(\theta) + \sin(\theta) \times \frac{1 - tg^2(\theta)}{2tg(\theta)} \right) \times \sin^2(2\theta) \times \frac{1}{2} + R\cos(\theta) = \quad \text{(A2.6)}$$

$$R\left(-\cos(\theta) + \sin(\theta) \times \frac{\left(1 - \frac{\sin^2(\theta)}{\cos^2(\theta)}\right)\cos(\theta)}{2\sin(\theta)} \right) \times (2\sin(\theta)\cos(\theta))^2 \times \frac{1}{2} + R\cos(\theta) = \quad \text{(A2.7)}$$

$$R\left(-\cos(\theta) + \frac{\cos^2(\theta) - \sin^2(\theta)}{2\cos(\theta)} \right) \times 4\sin^2(\theta)\cos^2(\theta) \times \frac{1}{2} + R\cos(\theta) = \quad \text{(A2.8)}$$

$$R\left(-2\cos^2(\theta)+(\cos^2(\theta)-\sin^2(\theta))\right)\times\sin^2(\theta)\cos(\theta)+R\cos(\theta)= \tag{A2.9}$$

$$R\left(-\cos^2(\theta)-\sin^2(\theta)\right)\times\sin^2(\theta)\cos(\theta)+R\cos(\theta)=-R\cos(\theta)\left(1-\sin^2(\theta)\right)=-R\cos^3(\theta) \tag{A2.10}$$

Finally, for $0\le\theta\le\Pi$ $\quad x(\theta)=|-R\cos^3(\theta)|=R\cos^3(\theta)$ (A2.11)

$$\lim_{d\to\infty} y(\theta)=tg\left(\arcsin\left(\frac{d\cos(\theta)}{\sqrt{R^2+d^2+2Rd\sin(\theta)}}\right)-\theta\right)(x-R\cos(\theta))-R\sin(\theta)= \tag{A2.12}$$

$$tg\left(\arcsin\left(\lim_{d\to\infty}\left(\frac{d\cos(\theta)}{\sqrt{R^2+d^2+2Rd\sin(\theta)}}\right)\right)-\theta\right)(x-R\cos(\theta))-R\sin(\theta)= \tag{A2.13}$$

$$tg(\arcsin(\cos(\theta))-\theta)\times(x-R\cos(\theta))-R\sin(\theta)= \tag{A2.14}$$

$$tg(\arcsin(\sin(\frac{\Pi}{2}-\theta))-\theta)\times(x-R\cos(\theta))-R\sin(\theta)=\frac{1}{tg(2\theta)}(x(\theta)-R\cos(\theta))-R\sin(\theta)= \tag{A2.15}$$

$$R\left(\frac{1}{tg(2\theta)}\left(\cos^3(\theta)-\cos(\theta)\right)-\sin(\theta)\right)=R\left(\frac{\cos(2\theta)}{\sin(2\theta)}\cos(\theta)\left(\cos^2(\theta)-1\right)-\sin(\theta)\right)= \tag{A2.16}$$

$$R\left(\frac{1-2\sin^2(\theta)}{2\sin(\theta)\cos(\theta)}\cos(\theta)\left(\cos^2(\theta)-\sin^2(\theta)-\cos^2(\theta)\right)-\sin(\theta)\right)=R\left(\frac{1-2\sin^2(\theta)}{2\sin(\theta)}(-\sin^2(\theta)-\sin(\theta)\right)= \tag{A2.17}$$

$$R\frac{-3\sin^2(\theta)+2\sin^4(\theta)}{2\sin(\theta)} \qquad \text{Finally,} \quad y(\theta)=\frac{R}{2}(2\sin^3(\theta)-3\sin(\theta)) \tag{A2.18, A2.19}$$

APPENDIX 3

Derivation of Eqs. (41), (42) (line A3.9)

$$\frac{d}{dt}p_{c,res}(t,\theta)=\frac{d}{dt}\left[\sqrt{\frac{I_o}{2\rho c}}\left(\sin(\varpi(t+\Delta t1))+\sqrt{\frac{2(1-\alpha)\sin(\theta)}{3|\cos^3(\theta)|}}\sin(\varpi(t+\Delta t_2))\right)\right]= \tag{A3.1}$$

$$\sqrt{\frac{I_o}{2\rho c}}\varpi\left(\cos(\varpi(t+\Delta t1))+\sqrt{\frac{2(1-\alpha)\sin(\theta)}{3|\cos^3(\theta)|}}\cos(\varpi(t+\Delta t_2))\right)=0$$

Substituton $\tau=t+\Delta t_1$ and $b=\sqrt{\frac{2(1-\alpha)\sin(\theta)}{3|\cos^3(\theta)|}}$ (A1.2), (A3.3)

yields $$\cos\varpi(\tau)=-b\ \cos\varpi(\tau-(\Delta t_1-\Delta t_2)) \tag{A3.4}$$

and after expansion $$\cos\varpi(\tau)=-b\left[\cos(\varpi\tau)\cos(\varpi(\Delta t_1-\Delta t_2))+\sin(\varpi\tau)\sin(\varpi(\Delta t_1-\Delta t_2))\right] \tag{A3.5}$$

Regrouping yields $$\frac{\sin(\varpi\tau)}{\cos(\varpi\tau)}=\frac{\frac{1}{b}+\cos(\varpi(\Delta t_1-\Delta t_2))}{\sin(\varpi(\Delta t_1-\Delta t_2))} \tag{A3.6}$$

and then $$\varpi(t+\Delta t_1)=\operatorname{arctg}\left(\frac{\frac{1}{b}+\cos(\varpi(\Delta t_1-\Delta t_2))}{\sin(\varpi(\Delta t_1-\Delta t_2))}\right) \tag{A3.7}$$

Since $$\Delta t_2-\Delta t_2=\frac{\frac{R}{2}(3\sin\theta-2\sin^3\theta)}{c}-\frac{\frac{R}{2}3\sin\theta}{c}=-\frac{R\sin^3\theta}{c}, \tag{A3.8}$$

$$t=\frac{1}{\varpi}\operatorname{arctg}\left(\frac{\sqrt{\frac{3|\cos^3\theta|}{2(1-\alpha)\sin\theta}}+\cos\left(\varpi\frac{R\sin^3\theta}{c}\right)}{\sin\left(\varpi\frac{R\sin^3\theta}{c}\right)}\right)-\Delta t_1 \tag{A3.9}$$

References

[1] Barron M., Auditorium acoustics and architectural design. E&FN Spon, London - New York (1998)

[2] Kulowski A., The caustic in the acoustics of historic interiors. Applied Acoustics **133**, 82–90 (2018)

[3] *http://www.bl.uk/turning-the-pages/?id=cb4c06b9-02f4-49af-80ce-540836464a46&type=book*, p.8-14 [23.06.2018]

[4] Shealy D. L., Burkhard D. G., Caustic Surfaces and Irradiance for Reflection and Refraction from an Ellipsoid, Elliptic Paraboloid, and Elliptic Cone. Applied Optics **12**, 2955-9 (1973)

[5] Кравцов Ю.А., Орлов Ю.И., Геометрическая опика неоднородных сред (Kravtcov Yu. A., Orlov Yu. I.: Geometric optics of inhomogeneous media, in Russian). Издательство "Наука", Москва, §4, §6 (1980)

[6] Paun B., Istraživanje kaustike metodom praćenja svjetlosnih zraka i usporedba s eksperimentom (Caustic research by the light rays tracing and experimental verification, in Croatian). Graduate work. University of Zagreb, Faculty of Science, Department of Physics, page 86. Zagreb (2011) *http://asiber.ifs.hr/bruno_pauns_caustic/BrunoPaun_diplomski_rad.pdf* [25.04.2018]

[7] Ivanov V.P., Ivanova G.K., Caustic structure of the underwater sound channel. Open Journal of Acoustics, **4,** 26-37 (2014) *http://file.scirp.org/pdf/OJA_2014032115460011.pdf* [02.05.2018].

[8] Khatkevich A. G., Khatkevich L. A., Propagation of laser beams and caustics in crystals. Journal of Applied Spectroscopy, **74**, No. 4 (2007) *https://link.springer.com/article/10.1007/s10812-007-0086-8* [02.05.2018].

[9] Skowron J. Analiza niestandardowych zjawisk mikrosoczewkowania grawitacyjnego gwiazd Galaktyki. Rozprawa doktorska (Analysis of non-standard phenomena of gravitational microlensing of Galactic stars. PhD dissertation, in Polish). Uniwersytet Warszawski (2009) *http://www.astrouw.edu.pl/~jskowron/PhD/thesis/phd.pdf* [21.09.2018]

[10] Castagnede B., Sahraoui S., Tournat V., Tahani N., Cuspidal caustic and focusing of acoustical waves generated by a parametric array onto a concave reflecting surface. C. R. Mecanique, **337**, 693-702 (2009)

[11] Kuttruff H., Room acoustics. Spon Press, London – New York, chap. 4.4 (2000) *https://danylastchild07.files.wordpress.com/2016/05/room-acoustics-kuttruff.pdf* [21.09.2018].

[12] Weisstein, E.W., Epicycloid. From MathWorld-A Wolfram Web Resource. *http://mathworld.wolfram.com/Epicycloid.html* [21.09.2018]

[13] *http://pl.easima.com* (2015) [21.09.2018]

[14] Burkhard D. G., Shealy D. L., Formula for the density of tangent rays over a caustic surface. Applied Optics vol. 21, No. 18, 3299-06 (1982)

[15] Cremer L., Müller H. A., Schultz T. J., Principles and application in room acoustics, Applied Science Publishers, London - New York, chap. 1. 1 (1982)

[16] Egan MD.: Concepts in architectural acoustics, McGraw-Hill Book Company, New York, 89–90 (1988)

[17] http://hyperphysics.phy-astr.gsu.edu/hbase/phyopt/Raylei.html [21.09.2019]

[18] *http://poznanfilmcommission.pl/lokacja/aula-uam* [21.09.2019]

[19] Fasold W., Winkler H., Bauphysikalische Entwurfslehre, Band 5. Raumakustik. VEB Verlag fur Bauwesen, Berlin, chap. 2.1.1.2 (1976)

[20] https://medievalheritage.eu/en/main-page/dictionary/barrel-vault/ [21.09.2019]

[21] https://commons.wikimedia.org/w/index.php?curid=4395135 [21.09.2019]

[22] https://commons.wikimedia.org/w/index.php?curid=23778427 [21.09.2019]

[23] *https://www.gdynia.pl/co-nowego,2774/muszla-koncertowa-ma-swojego-inwestora,496574* [21.09.2018]